SÍSMICA 2024
13º Congresso Nacional de Sismologia e Engenharia Sísmica

OPTIMAL INTENSITY MEASURES FOR PROBABILISTIC SEISMIC DEMAND MODELS OF HISTORICAL MASONRY BUILDINGS CONSIDERING IN-PLANE AND OUT-OF-PLANE RESPONSE

DANIEL CAICEDO
PhD Candidate
Department of Civil Engineering, Institute for Sustainability and Innovation in Structural Engineering, (ISISE), ARISE, University of Minho, Guimarães, Portugal

SHAGHAYEGH KARIMZADEH
Postdoctoral research
Department of Civil Engineering, Institute for Sustainability and Innovation in Structural Engineering, (ISISE), ARISE, University of Minho, Guimarães, Portugal

VASCO BERNARDO
Postdoctoral research
Department of Civil Engineering, Institute for Sustainability and Innovation in Structural Engineering, (ISISE), ARISE, University of Minho, Guimarães, Portugal

PAULO B. LOURENÇO
Full Professor
Department of Civil Engineering, Institute for Sustainability and Innovation in Structural Engineering, (ISISE), ARISE, University of Minho, Guimarães, Portugal

ABSTRACT

This research focuses on the identification of optimal Intensity Measures (IMs) for the probabilistic seismic demand analysis of historical masonry buildings. Two case study structures are modelled in the OpenSees environment using three-dimensional macroelements that consider both the in-plane and out-of-plane response of masonry walls. A large set of real accelerograms is selected using unconditional selection, i.e., non-dependent from structural periods. After conducting non-linear time history analyses, IMs are ranked according to the notions of efficiency, practicability, proficiency, and sufficiency. Further, a composed measure is proposed as a combination of the IMs that exhibit the best coefficient of determination (R^2) within the IM vs. Engineering Demand Parameter (EDP) regression. Consistent Probabilistic Seismic Demand Models (PSDMs) and fragility curves are derived from cloud analysis afterwards.

KEYWORDS: Probabilistic seismic demand model, Historical masonry buildings, Out-of-plane response, Fragility curves.

1. INTRODUCTION

Historical masonry buildings, which can be found throughout Europe, are vulnerable structures that can be severely affected by earthquake ground motions. On top of that, the majority of these structures represent cultural heritage, for which it is necessary to adopt competent tools to assess seismic vulnerability. In this regard, Performance-based earthquake engineering (PBEE) can be adopted for the prediction of the performance of complex structures at different levels of damage state (DS) [1,2]. Moreover, Probabilistic Seismic Demand Analysis (PSDA) has become an important element of seismic risk mitigation and decision-making in the context of PBEE [3].

The basis of PSDA and associated Probabilistic Seismic Demand Models (PSDMs) have been thoroughly discussed in [4,5]. The ultimate outcome of PSDA is a seismic fragility curve and the selection of optimal IM parameters. Besides seminal works oriented to building structures [6,7], bridges [8,9], or concrete dams [10], other structure typologies have been approached in this framework, including transmission towers [11], pile group-supported bridges [12], open-pit slopes [13], and concrete face rockfill dams [14]. Specifically, Vargas-Alzate et al. [15] examined the accuracy of IMs in predicting the seismic response of building classes considering near- and far-fault ground motions. Recently, Guo et al. [16] proposed a general procedure to identify the optimal IMs for long span cable-stayed bridges based on generalized linear regression models.

This study aims to identify optimal IMs to develop PSDMs of Historical masonry buildings. The nonlinear numerical models of two case study buildings, representative of stiff monumental masonry structures and tall and slender residential masonry buildings, are developed in the OpenSees software package [17]. A set of 100 ground motion records, classified according to their IMs, are utilized to perform nonlinear time history analyses. Optimal IMs are evaluated based on statistical indicators of PSDMs, which are the coefficient of determination, dispersion, practicality, and proficiency. In addition, Lasso regression [18] is adapted to derive a composed metric (Icomp) that better describes the seismic behaviour of historical masonry buildings as a linear combination of the IMs with the best correlation. Finally, cloud-based fragility curves are drawn to compare the performance of Icomp in the seismic fragility analysis of masonry structures against individual IMs.

2. CASE STUDIES DEFINITION AND NUMERICAL MODELLING

2.1. Description of the buildings' topology

The Holsteiner Hof building is a 2-storey stone masonry building representing stiff monumental heritage structures. The building has a regular rectangular plan with dimensions of 26.00 m × 14.00 m. The height of each storey is 4.50 m. The wall and spandrels thicknesses are 60 cm and 30 cm, respectively. Triangular gables at the top have a thickness of 45 cm. The floor system is composed of timber beams, simply supported on the walls in the shorter direction, and a layer of planks nailed directly to the beams. Hence, horizontal forces are assumed to be transferred as friction forces. The roof system is composed of a wooden truss structure. Minor retrofitting interventions were reported during 1976–1979 that, in general, did not modify the structural system.

On the other hand, the Lausanne Malley is a 6-storey structure representative of tall and slender residential masonry buildings. The building is regular in plan with dimensions of 14.00 m × 12.00 m. The storey height oscillates within the range of 2.80 − 3.20 m. Accordingly, the wall thickness varies from 60 to 25 cm, along with the height of the building. The floor system is composed of timber beams, simply supported on the walls in the shorter direction, and a layer of planks nailed directly to the beams. Thus, as with the Holsteiner Hof building, the horizontal forces are transferred as friction forces. The

roof system is composed of a wooden truss structure. Seismic retrofit of the building was reported recently in [19].

2.2. Modelling approach

Both structures are modelled in OpenSees [17] using 3D macroelements [20] to account for IP and OOP effects. The macroelement is formulated as a one-dimensional element with two nodes at the element ends and one additional node at the midspan. The element is able to capture the IP and OOP response through three sectional models applied at the element ends and at the central section (P-Δ formulation is considered to capture the nonlinear geometrical effects). Drift values can be calculated individually for flexural and shear deformations by considering the rotations and lumped shear deformations at the central node. Exceeding the limits in drift values will lead to the loss of lateral strength of the element.

The floor system is modelled using orthotropic elastic membranes with higher stiffness in the direction of the beam span and lower stiffness in the other direction (i.e., membrane definition is given by the two moduli of elasticity in the orthogonal directions, shear modulus, and thickness of the diaphragm). Floor-to-wall connections are modelled to account for nonlinear behaviour and potential connection failure at the beam support that can result in the OOP failure of a pier element. Likewise, zero-length elements are used to model the frictional interfaces and possible relative displacement between the nodes. A zero-length wall-to-wall interface with linear elastic behaviour in compression, no crushing, and a finite tensile strength with exponential softening is used to simulate the formation of vertical cracks and separation of the orthogonal walls due to poor interlocking, which might lead to potential OOP failure of the macroelement.

A 5% proportional Rayleigh damping is assumed within the non-linear dynamic simulations, and a secant stiffness damping model is adopted to avoid overdamping in the OOP failure mechanism and to capture the full OOP rocking response. Table 1 summarizes the Modelling parameters adopted as the mean or median values reported by Tomić et al [21]. The symbol (*) over the values in the third column of Table 1 denotes the median value taken from a lognormal distribution. Fig. 1 illustrates the numerical models of the Holsteiner Hof and Lausanne Malley buildings, respectively, as well as their first three vibration periods.

Table 1- Masonry and modelling parameters.

Parameter	Definition	Mean value
	Masonry Parameters	
E_m [Pa]	Modulus of elasticity [22–24]	3.5 × 109
G_m [Pa]	Shear modulus [22–24]	1.5 × 109*
f'_{cm} [Pa]	Compressive strength [22–24]	1.3 × 106
c_m [Pa]	Cohesion [22–24]	2.33 × 105*
μ_m [-]	Friction coefficient [22–24]	0.25*
ρ [kg]	Density [22–24]	2000
	Modelling Parameters	
k_{floor} [-]	Floor stiffness factor [25,26]	1*
f_w [-]	Wall-to-wall connection factor [27]	1*
$\mu_{f\text{-}w}$ [-]	Floor-to-wall friction coefficient [28,29]	1*
$\delta_{c,flexure}$ [-]	Drift capacity in flexure [30]	0.01035*
$\delta_{c,shear}$ [-]	Drift capacity in Shear [30]	0.007*
ζ [-]	Damping ratio [28]	0.05

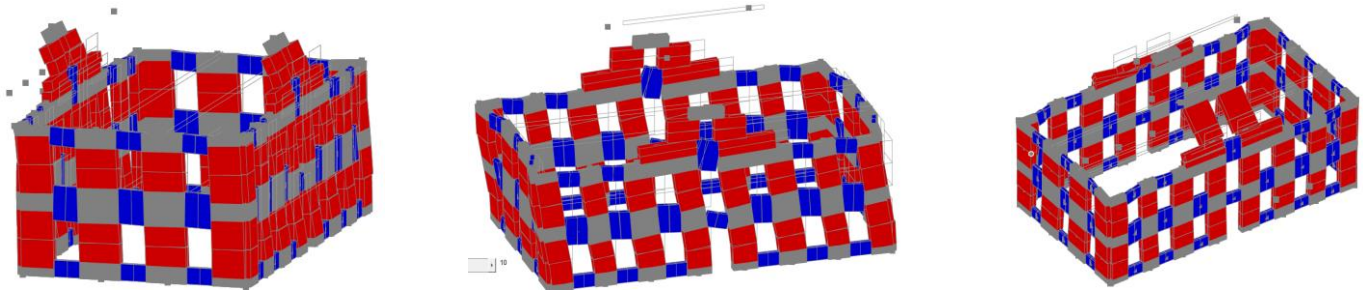

(a) Holsteiner Hof, T1 = 0.16 s. (b) Holsteiner Hof, T2 = 0.14 s. (c) Holsteiner Hof, T3 = 0.12 s.

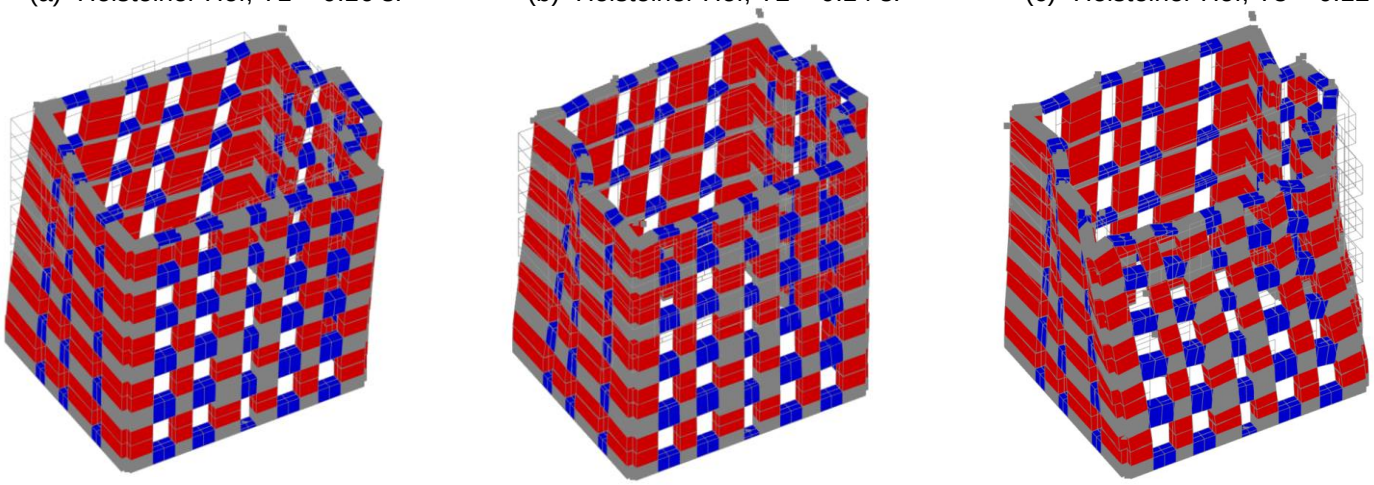

(d) Lausanne Malley, T1 = 0.50 s. (e) Lausanne Malley, T2 = 0.42 s. (f) Lausanne Malley, T3 = 0.33 s.

Fig. 1 - Numerical models and fundamental vibration periods.

3. SEISMIC INPUT DEFINITION

Unconditional selection [31], independent from structural periods, was adopted to select 100 accelerograms as seismic input for the PSDMs. The seismological parameters for selection are set as: 4.5 ≤ Mw ≤ 7.8; 90 m/s ≤ Vs30 ≤ 1050 m/s; RJB ≤ 185 km. Fig. 2 shows the 5% damped geometric mean spectral acceleration (S_a) of the selected records alongside the mean, median, and 95% confidence interval. All accelerograms are classified according to their seismological characteristics and IMs. A classification similar to the one presented by Hariri-Ardebili and Saouma [10] is adopted to subdivide IMs into period and duration-related, ground motion dependent scalars, ground motion dependent compound, structure-independent spectral, and structure-dependent spectral IMs.

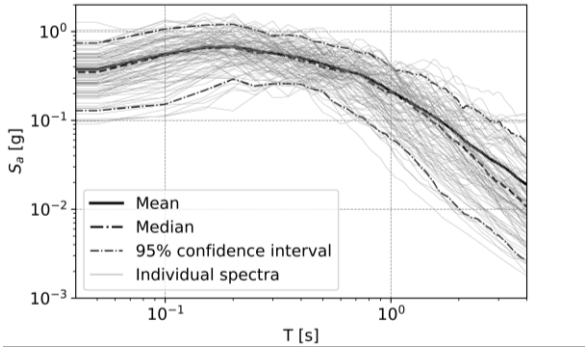

Fig. 2 - 5% damped geometric mean Sa of selected records.

4. PROBABILISTIC SEISMIC DEMAND MODELS

PSDMs refer to the conditional probability of an EDP reaching or exceeding a certain level of *edp*, given a seismic IM level, i.e., P(EDP ≥ *edp* | IM). As specified by Cornell et al. [32] the median seismic demand *vs.* IM regression ($\eta_{EDP|IM}$) normally follows a power-law function, linear in the logarithmic scale. Thus, the form and logarithmic standard deviation ($\beta_{EDP|IM}$) of the assumed PSDM can be described through the following set of equations:

$$\eta_{EDP|IM} = a\ IM^{b} \tag{1}$$

$$\beta_{EDP|IM} \cong \sqrt{\frac{\sum_{i=1}^{n} (\ln edp_i - \ln \eta_{EDP|IM})^2}{n-2}} \tag{2}$$

where *a* and *b* are the regression constants; and *n* is the total number of ground motion considered for the non-linear time history analyses.

Additionally, a composed measure (I_{comp}) is proposed as a linear combination of the IMs that exhibit the best R^2 within the EPD *vs*. IM regression. Lasso regression [18] is adapted to identify the necessary IMs, and then derive the optimal I_{comp} that best describes the dynamic response of the masonry buildings in terms of EDPs. Equation (3) defines the cost function to minimize in the Lasso regression:

$$f(\theta) = \sum_{i=1}^{m} (y_i - \boldsymbol{x}_i^T \boldsymbol{\theta})^2 + \lambda \sum_{i=1}^{m} |\theta_i| \tag{3}$$

where $\boldsymbol{\theta} = [\theta_1, \theta_2, \ldots, \theta_n]^T$ is the regression coefficient vector; $\boldsymbol{x}_i = [x_{i1}, x_{i2}, \ldots, x_{in}]^T$ is the i^{th} input variable vector; y_i is the i^{th} observed response; and λ is a positive number that controls the shrinkage, so the larger the value of λ, the greater the amount of shrinkage. Hence, the formulation for I_{comp} is given as:

$$I_{comp} = \prod_{i=1}^{m} IM_i^{\theta_i} \tag{4}$$

with *m* as the number of relevant IMs for the structure under analysis, recognised as those that exhibit the best correlation in the EPD *vs*. IM regression ($R^2 \geq 0.6$ is assumed). In this regard, Table 2 delivers the information from the PSDMs for individual IMs alongside the values from the assessment of IMs in terms of efficiency, practicability, proficiency, and sufficiency [33]. IMs are sorted from the lowest to the highest dispersion, $\beta_{EDP|IM}$, i.e., the most efficient to the least efficient one. Only IMs with $R^2 \geq 0.6$ are reported since they are preselected for the derivation of I_{comp} afterwards. The preselected IMs for the Holsteiner Hof building correspond to Peak Ground Acceleration, PGA; Effective Peak Acceleration, EPA; Improve Effective Peak Acceleration, IEPA [34]; Acceleration Spectrum Intensity [35], ASI; Cordova intensity [36], S_a^*; and Vamvatsikos intensity [37], either $\overline{S_a}$ or $\overline{\overline{S_a}}$. In the case of the Lausanne Malley the preselected IMs correspond to Peak Ground Velocity, PGV; Modified Acceleration Spectrum Intensity [38], ASI*; Velocity Spectrum Intensity, VSI; spectral acceleration, velocity, and displacement at the fundamental period T1, $S_a(T_1)$, $S_v(T_1)$, $S_d(T_1)$, respectively; and S_a^*, $\overline{S_a}$, and $\overline{\overline{S_a}}$.

In general, it is observed how the values of modified dispersion, ζ, follow the same ascending trend as $\beta_{EDP|IM}$, denoting from the most to least proficient IMs. Inversely, correlation values, R^2, decrease as the values of ζ and $\beta_{EDP|IM}$ increase. The preselected IMs for the Holsteiner Hof building correspond to acceleration-related metrics, which is consistent with the behaviour of short-period structures [39]. In contrast, the analysis of the Lausanne Malley building pointed out to a combination of acceleration, velocity and

(c) ln(max($\bar{\Delta}_r$)) *vs.* ln(I_{comp}) — Lausanne Malley building

(d) ln(max(V_b)) *vs.* ln(I_{comp}) — Lausanne Malley building

Fig. 3 portrays the PSDMs derived after I_{comp} for both global metrics under analysis (i.e., maximum average roof displacement, max($\bar{\Delta}_r$); and maximum base shear, max(V_b)). A considerable improvement is observed for the derived PSDMs in terms of correlation, efficiency, practicability, and proficiency.

Table 2 - Optimal IM assessment.

EDP			max($\bar{\Delta}_r$)				EDP			max(V_b)			
IM	b	$\beta_{EDP\|IM}$	ζ	R^2	*p-value*		IM	b	$\beta_{EDP\|IM}$	ζ	R^2	*p-value*	
					M_w	R_{JB}						M_w	R_{JB}
Holsteiner Hof													
EPA	2.00	0.40	0.20	0.73	0.24	0.38	EPA	0.66	0.11	0.17	0.80	0.14	0.89
ASI	2.00	0.40	0.20	0.73	0.24	0.38	ASI	0.66	0.11	0.17	0.80	0.14	0.89
S_a^*	1.72	0.43	0.25	0.68	0.11	0.15	$\overline{\overline{S_a}}$	0.59	0.11	0.19	0.78	0.09	0.62
$\overline{\overline{S_a}}$	1.75	0.43	0.25	0.69	0.17	0.30	IEPA	0.62	0.12	0.20	0.74	0.10	0.83
IEPA	1.75	0.49	0.28	0.60	0.21	0.81	S_a^*	0.55	0.14	0.25	0.69	0.08	0.54
PGA	1.46	0.50	0.35	0.57	0.01	0.09	$\overline{S_a}$	0.48	0.14	0.29	0.68	0.01	0.34
$\overline{S_a}$	1.34	0.52	0.39	0.54	0.04	0.30	PGA	0.49	0.15	0.30	0.63	0.00	0.21
Lausanne Malley													
$S_a(T_1)$	1.08	0.26	0.24	0.75	0.36	0.71	PGV	0.45	0.15	0.33	0.66	0.00	0.00
$S_d(T_1)$	1.08	0.26	0.24	0.75	0.36	0.70	ASI*	0.50	0.16	0.32	0.61	0.01	0.00
$S_v(T_1)$	1.18	0.27	0.23	0.72	0.20	0.70	$S_v(T_1)$	0.51	0.16	0.31	0.59	0.36	0.02
$\overline{S_a}$	0.99	0.27	0.27	0.73	0.44	0.07	VSI	0.39	0.17	0.44	0.52	0.01	0.00
PGV	0.91	0.31	0.34	0.63	0.64	0.66	$S_a(T_1)$	0.44	0.17	0.40	0.52	0.36	0.01
ASI*	1.06	0.31	0.29	0.65	0.78	0.89	$S_d(T_1)$	0.43	0.17	0.40	0.52	0.36	0.01
S_a^*	0.83	0.31	0.38	0.63	0.79	0.10	$\overline{S_a}$	0.40	0.18	0.44	0.50	0.05	0.00
VSI	0.87	0.32	0.37	0.61	0.37	0.19	S_a^*	0.34	0.19	0.55	0.44	0.12	0.00
$\overline{\overline{S_a}}$	0.82	0.32	0.39	0.62	0.60	0.07	$\overline{\overline{S_a}}$	0.33	0.19	0.57	0.43	0.08	0.00

Now, PSDM-based fragility curves, obtained after the aggregation of the results from cloud analysis, are derived to examine the effect of I_{comp} in the seismic fragility analysis of masonry structures. Fig. 4 presents the fragility curves for both case study buildings at collapse DS considering the standardized values of IM through min-max normalization. Collapse DS is defined by values of max($\bar{\Delta}_r$) larger than 40 mm and 45 mm for the Holsteiner Hof building and the Lausanne Malley building, respectively. For the Holsteiner Hof building, the prediction of collapse is less conservative using the I_{comp} as the independent variable, and its performance is comparable with the results of S_a^*, $\overline{S_a}$, $\overline{\overline{S_a}}$, and PGA. Conversely, for the Lausanne Malley building, the prediction of collapse is similar for any of the assessed IMs, being the prediction computed through I_{comp} approximately on the average of all IMs.

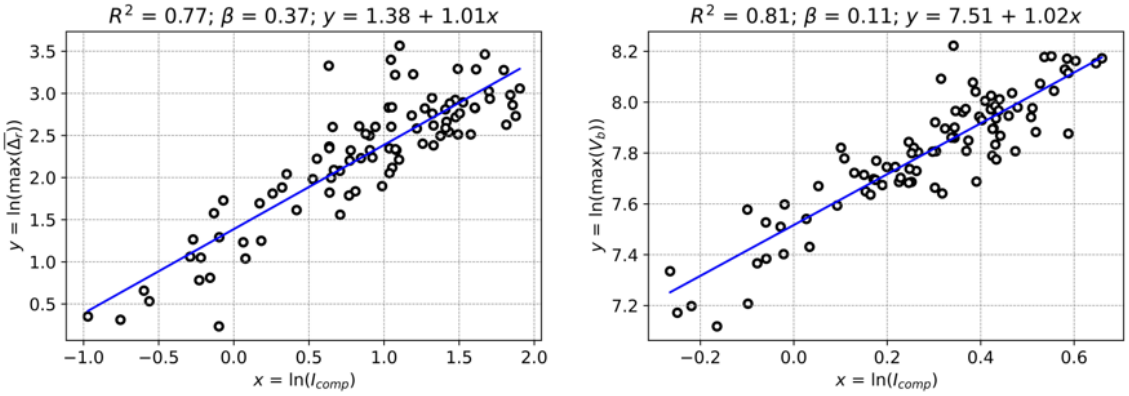

(a) ln(max($\overline{\Delta}_r$)) *vs.* ln(I_{comp}) — Holsteiner Hof building

(b) ln(max(V_b)) *vs.* ln(I_{comp}) — Holsteiner Hof building

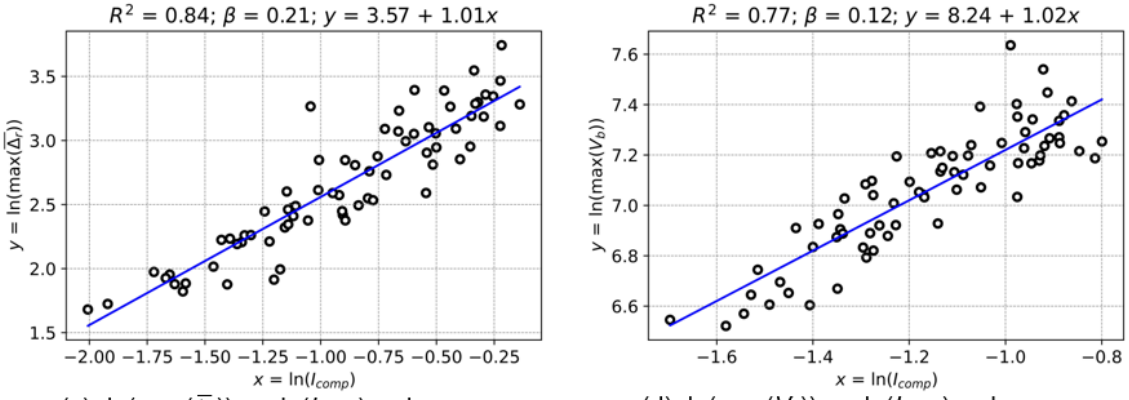

(c) ln(max($\overline{\Delta}_r$)) *vs.* ln(I_{comp}) — Lausanne Malley building

(d) ln(max(V_b)) *vs.* ln(I_{comp}) — Lausanne Malley building

Fig. 3 - PSDM with Icomp as independent variable.

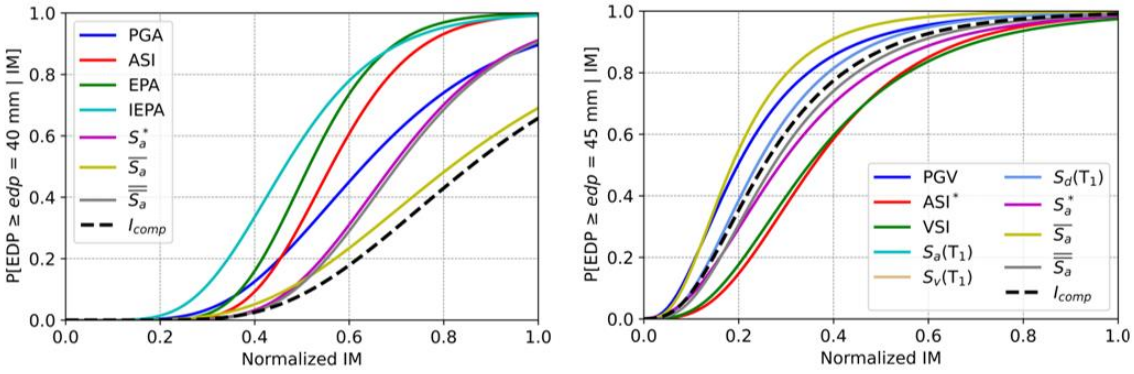

(a) Holsteiner Hof building

(b) Lausanne Malley building

Fig. 4 - Normalized fragility curves at collapse DS.

5. CONCLUSIONS

The identification of optimal IMs and derivation of an I_{comp} for the PSDA of historical masonry buildings were addressed in this research. Two case study buildings were modelled in OpenSees using 3D macroelements to account for IP and OOP effects. Within the PSDMs, IMs were ranked according to the notions of efficiency, practicability, proficiency, and sufficiency. IMs with the highest R^2 were preselected to derive an I_{comp} with better correlation, efficiency, practicability, and proficiency, adopting a machine learning approach based on Lasso regression. Further, the performance of individual IMs and I_{comp} was compared through cloud-based fragility analysis. Particularly, for the Holsteiner Hof building the preselected IMs correspond to acceleration-related metrics, while for the Lausanne Malley building, preselected IMs corresponded to a combination acceleration, velocity and displacement-related IMs. Regardless of the case study building, the I_{comp} metric demonstrated large improvements in terms of correlation, efficiency, practicability, and proficiency. Thus, the proposed framework led successfully to the identification of optimal IMs for the PSDA of historical masonry buildings. In future scenarios, the proposed methodology should be tested in the analysis masonry archetypes.

6. FUNDING

This work was partly financed by FCT/MCTES through national funds (PIDDAC) under the R&D Unit ISISE under reference UIDB/04029/2020, and under the Associate Laboratory Advanced Production and Intelligent Systems ARISE under reference LA/P/0112/2020. This study has been partly funded by the STAND4HERITAGE project that has received funding from the European Research Council (ERC) under the European Union's Horizon 2020 research and innovation program (Grant agreement No. 833123), as an Advanced Grant. This work is partly financed by national funds through FCT - Foundation for Science and Technology, under grant agreement 2023.01101.BD attributed to the first author.

7. REFERÊNCES

[1] Naeim F, Bhatia H, Lobo RM. Performance based seismic engineering. The Seismic Design Handbook 2001:757–92.
[2] Kramer SL. Performance-based earthquake engineering: opportunities and implications for geotechnical engineering practice. Geotechnical Earthquake Engineering and Soil Dynamics IV 2008:1–32.
[3] Xiao-hui YU, Guang-yuan W. Discussions on probabilistic seismic demand models. 工程力学 2013;30:172–9.
[4] Shome N. Probabilistic seismic demand analysis of nonlinear structures. Stanford University; 1999.
[5] Luco N. Probabilistic seismic demand analysis, SMRF connection fractures, and near-source effects. Stanford University; 2002.
[6] Barroso LR, Winterstein S. Probabilistic seismic demand analysis of controlled steel moment-resisting frame structures. Earthq Eng Struct Dyn 2002;31:2049–66.
[7] Freddi F, Padgett JE, Dall'Asta A. Probabilistic seismic demand modeling of local level response parameters of an RC frame. Bulletin of Earthquake Engineering 2017;15:1–23.
[8] Mackie K, Stojadinović B. Probabilistic seismic demand model for California highway bridges. Journal of Bridge Engineering 2001;6:468–81.
[9] Tondini N, Stojadinovic B. Probabilistic seismic demand model for curved reinforced concrete bridges. Bulletin of Earthquake Engineering 2012;10:1455–79.

[10] Hariri-Ardebili MA, Saouma VE. Probabilistic seismic demand model and optimal intensity measure for concrete dams. Structural Safety 2016;59:67–85.
[11] Tian L, Pan H, Ma R. Probabilistic seismic demand model and fragility analysis of transmission tower subjected to near-field ground motions. J Constr Steel Res 2019;156:266–75.
[12] Zhou L, Alam MS, Wang X, Ye A, Zhang P. Optimal intensity measure selection and probabilistic seismic demand model of pile group supported bridges in sandy soil considering variable scour effects. Ocean Engineering 2023;285:115365.
[13] Che W, Chang P, Wang W. Optimal Intensity Measures for Probabilistic Seismic Stability Assessment of Large Open-Pit Mine Slopes under Different Mining Depths. Shock and Vibration 2023;2023.
[14] Khalid MI, Park D, Fei J, Nguyen V-Q, Nguyen D-D, Chen X. Selection of efficient earthquake intensity measures for evaluating seismic fragility of concrete face rockfill dam. Comput Geotech 2023;163:105721.
[15] Vargas-Alzate YF, Hurtado JE. Efficiency of intensity measures considering near- and far-fault ground motion records. Geosciences (Basel) 2021;11:234.
[16] Guo J, Alam MS, Wang J, Li S, Yuan W. Optimal intensity measures for probabilistic seismic demand models of a cable-stayed bridge based on generalized linear regression models. Soil Dynamics and Earthquake Engineering 2020;131:106024.
[17] McKenna F. OpenSees: a framework for earthquake engineering simulation. Comput Sci Eng 2011;13:58–66.
[18] Tibshirani R. Regression shrinkage and selection via the lasso. J R Stat Soc Series B Stat Methodol 1996;58:267–88.
[19] Michel C, Karbassi A, Lestuzzi P. Evaluation of the seismic retrofitting of an unreinforced masonry building using numerical modeling and ambient vibration measurements. Eng Struct 2018;158:124–35.
[20] Vanin F, Penna A, Beyer K. A three-dimensional macroelement for modelling the in-plane and out-of-plane response of masonry walls. Earthq Eng Struct Dyn 2020;49. https://doi.org/10.1002/eqe.3277.
[21] Tomić I, Vanin F, Beyer K. Uncertainties in the seismic assessment of historical masonry buildings. Applied Sciences 2021;11:2280.
[22] Guerrini G, Senaldi I, Scherini S, Morganti S, Magenes G. Material characterization for the shaking-table test of the scaled prototype of a stone masonry building aggregate. Material Characterization for the Shaking-Table Test of the Scaled Prototype of a Stone Masonry Building Aggregate 2017:105–15.
[23] Senaldi I, Guerrini G, Scherini S, Morganti S, Magenes G, Beyer K, et al. Natural stone masonry characterization for the shaking-table test of a scaled building specimen. Proceedings of the International Masonry Society Conferences, vol. 0, 2018.
[24] Guerrini G, Senaldi I, Graziotti F, Magenes G, Beyer K, Penna A. Shake-Table Test of a Strengthened Stone Masonry Building Aggregate with Flexible Diaphragms. International Journal of Architectural Heritage 2019;13. https://doi.org/10.1080/15583058.2019.1635661.
[25] Brignola A, Podestà S, Pampanin S. In-plane stiffness of wooden floor. 2008 NZSEE Conference, Paper 49 2008.
[26] Brignola A, Pampanin S, Podestà S. Experimental evaluation of the in-plane stiffness of timber diaphragms. Earthquake Spectra 2012;28:1687–709.
[27] POLIMI. Critical Review of Methodologies and Tools for Assessment of Failure Mechanisms and Interventions, Deliverable 3.3, Workpackage 3: Damage Based Selection Of Technologies 2010.
[28] Vanin F, Penna A, Beyer K. Equivalent-Frame Modeling of Two Shaking Table Tests of Masonry Buildings Accounting for Their Out-Of-Plane Response. Front Built Environ 2020;6. https://doi.org/10.3389/fbuil.2020.00042.
[29] Almeida JP, Beyer K, Brunner R, Wenk T. Characterization of mortar–timber and timber–timber cyclic friction in timber floor connections of masonry buildings. Materials and Structures/Materiaux et Constructions 2020;53. https://doi.org/10.1617/s11527-020-01483-y.

[30] Vanin F, Zaganelli D, Penna A, Beyer K. Estimates for the stiffness, strength and drift capacity of stone masonry walls based on 123 quasi-static cyclic tests reported in the literature. Bulletin of Earthquake Engineering 2017;15. https://doi.org/10.1007/s10518-017-0188-5.
[31] Jayaram N, Lin T, Baker JW. A Computationally efficient ground-motion selection algorithm for matching a target response spectrum mean and variance. Earthquake Spectra 2011;27. https://doi.org/10.1193/1.3608002.
[32] Cornell CA, Jalayer F, Hamburger RO, Foutch DA. Probabilistic basis for 2000 SAC federal emergency management agency steel moment frame guidelines. Journal of Structural Engineering 2002;128:526–33.
[33] Giovenale P, Cornell CA, Esteva L. Comparing the adequacy of alternative ground motion intensity measures for the estimation of structural responses. Earthq Eng Struct Dyn 2004;33:951–79.
[34] Council AT, California SEA of. Tentative Provisions for the Development of Seismic Regulations for Buildings: A Cooperative Effort with the Design Professions, Building Code Interests, and the Research Community. Department of Commerce, National Bureau of Standards; 1978.
[35] von Thun JL, Roehm LH, Scott GA, Wilson JA. Earthquake ground motions for design and analysis of dams. Earthquake Engineering and Soil Dynamics II - Recent Advances in Ground-Motion Evaluation: Proceedings of the Specialty Conference, 1988.
[36] Cordova PP, Deierlein GG, Mehanny SSF, Cornell CA. Development of a two-parameter seismic intensity measure and probabilistic assessment procedure. The second US-Japan workshop on performance-based earthquake engineering methodology for reinforced concrete building structures, vol. 20, 2000, p. 0.
[37] Vamvatsikos D, Cornell CA. Developing efficient scalar and vector intensity measures for IDA capacity estimation by incorporating elastic spectral shape information. Earthq Eng Struct Dyn 2005;34:1573–600.
[38] Yakut A, Yılmaz H. Correlation of deformation demands with ground motion intensity. Journal of Structural Engineering 2008;134:1818–28.
[39] Chopra AK. Dynamics of structures. Pearson Education India; 2007.